Compensation of the negative effects of micro-encapsulated phase change materials by incorporating metakaolin in geopolymers based on blast furnace slag

Bouha El Moustapha, Stéphanie Bonnet, Abdelhafid Khelidj, Nordine Leklou, Daniel Froelich, Isselmou Ahmedou Babah, Carole Charbuillet, Abderahmane Khalifa

▶ **To cite this version:**

Bouha El Moustapha, Stéphanie Bonnet, Abdelhafid Khelidj, Nordine Leklou, Daniel Froelich, et al.. Compensation of the negative effects of micro-encapsulated phase change materials by incorporating metakaolin in geopolymers based on blast furnace slag. Construction and Building Materials, 2022, 314, part B, pp.125556. 10.1016/j.conbuildmat.2021.125556 . hal-04568867

HAL Id: hal-04568867
https://hal.science/hal-04568867

Submitted on 6 May 2024

HAL is a multi-disciplinary open access archive for the deposit and dissemination of scientific research documents, whether they are published or not. The documents may come from teaching and research institutions in France or abroad, or from public or private research centers.

L'archive ouverte pluridisciplinaire **HAL**, est destinée au dépôt et à la diffusion de documents scientifiques de niveau recherche, publiés ou non, émanant des établissements d'enseignement et de recherche français ou étrangers, des laboratoires publics ou privés.

Compensation of the negative effects of micro-encapsulated phase change materials by incorporating metakaolin in geopolymers based on blast furnace slag

Bouha EL MOUSTAPHA[1,2,3,*], Stéphanie BONNET[2], Abdelhafid KHELIDJ[2], Nordine LEKLOU[2], Daniel FROELICH[1] , Isselmou AHMEDOU BABAH[3] , Carole CHARBUILLET[1], Abderahmane KHALIFA[4]

* Corresponding Author

[1]Arts & Métiers sciences and technologies —Innovation and Product Design Laboratory, 151 Boulevard de l'Hôpital, F-75013 Paris, France.

[2] University of Nantes - IUT Saint-Nazaire, GeM, CNRS UMR 6183, Research Institute in Civil Engineering and Mechanics, 58 rue Michel Ange (BP 420), 44606 Saint Nazaire Cedex, France.

[3] University of Nouakchott AL-Aasriya , Faculty of Sciences and Techniques/UCME, BP 880, Nouakchott, Mauritanie.

[4]MAGMA group laboratory (www.magma-groupe.com), villa 051 bis-BP 2942- Nouakchott – Mauritania.

Corresponding author e-mail: Bouha.el_moustapha@ensam.eu

HIGHLIGHTS

- Geopolymer-MPCM mortars have shown better mechanical performance compared to Portland cement-MPCM mortars.
- The CASH and NASH gels formed after the inclusion of metakaolin also improved the mechanical and thermal performance of the geopolymer-MPCM mortars.

- Good linear correlations were obtained between compressive strengths on the one hand and Young's modulus and thermal conductivity on the other.

Abstract

This study aims to use NASH (sodium alumina silicate hydrate) gel and CASH (calcium alumina silicate hydrate) gel to overcome the negative effects of incorporating microencapsulated phase change materials (MPCM) on the mechanical strength and thermal conductivity of blast furnace slag-based geopolymer mortars. The coexistence of CASH and NASH gels was obtained by using an inclusion of a small amount of metakaolin in a geopolymer matrix based on blast furnace slag; this results in a geopolymer with high mechanical strength. Several tests were performed to characterize different mortars (with and without MK) such as workability, microstructural properties, water porosity, mechanical properties (compressive strength, dynamic Young modulus) and thermal properties (thermal conductivity, the specific heat capacity). The results obtained showed that the coexistence of NASH and CASH gel brought improvements in terms of mechanical properties and thermal conductivity compared to GBFS-based geopolymer-MPCM only. Indeed, the addition of 10 and 20% of metakaolin was sufficient to obtain this coexistence. With a concentration of MPCM up to 10% in the geopolymer mortars, the compressive strength was increased by about 10 MPA and the thermal conductivity was increased by about 31%, which led to an improvement in the specific heat capacity of up to 1280 J/Kg.K. These improvements were due to the high reactivity of MK under the activation conditions used. This favored the good dissolution of silica and aluminum in the MK, which participated well with the calcium in the GBFS to create the NASH and CASH gels. In fact, it was felt that these two gels filled the small pores caused by the MPCM and that this compensated well for their negative effects on the geopolymer matrix.

Geopolymer-MPCM based mortars after their optimizations with NASH and CASH gel coexistence showed good workability, compressive strength, and thermal performance. On the other hand, a reduced water porosity compared to Portland cement-MPCM based mortars.

Keywords: Geopolymer; Microcapsule Phase Change Materials; Granulated Blast Furnace Slag; Metakaolin

1. Introduction

The building sector is the world's largest energy consumer, consuming 36% of the world's total final energy and emitting more than 40% of total direct and indirect carbon dioxide (CO_2) emissions [1]. Most of the energy consumption in the building is reserved for thermal comfort improvement in the hot and cold seasons (building use phase) [2]. Furthermore, 80% of the greenhouse gas emissions are related to this phase [3].

Several researchers in recent decades have studied thermal storage through latent heat in order to reuse it when the building needs the heat (e.g., store heat during the day and use it at night) [4–6]. Among the techniques to improve thermal comfort is the use of Microencapsulated Phase Change Materials (MPCM). These materials help to regulate heat exchange in building compartments and reduce the requirement for heating and cooling systems [4–8]. MPCM store at a constant temperature (ambient temperature around human comfort) a large amount of energy in the form of latent heat during their phase change (solid liquid), which prevents the heat flow from entering the building during peak hours. This amount of heat is stored during the day and released at night [9]. This technology ensures the desired thermal comfort and reduces the need for air conditioning and heating, as well as reducing CO_2 emissions related to energy consumption in the building. A recent literature review showed that the use of these materials in buildings reduces annual energy consumption by about 50% for cooling and heating [2].

After mentioning the enormous energy consumption of the building sector, there is also another problem in this sector, namely is the massive use of Portland cement in concrete. The cement

industry is responsible for 7% of the world's CO_2 emissions [10] and causes other pollution in the air, water, etc.

The reflection of a strategy to reduce the environmental impacts related to CO_2 emissions and the improvement of the durability of concrete encouraged the researcher Davidovits [11] to invent a new ecological cement (with less environmental impacts) called the Geopolymer. This material is the result of the activation of aluminosilicate materials by alkaline solutions [11]. Aluminosilicate materials are industrial wastes, by-products, or types of clays such as Granulated Blast Furnace Slag (GBFS), metakaolin (MK), fly ash, and red mud, etc. The use of these materials to replace Portland cement will reduce CO_2 emissions and waste caused by the industries, thus helping to reduce the impact on the environment. Wang et al. [12] showed that the CO_2 emissions caused by the production of geopolymer are reduced by about 70 to 80% compared to the production of clinker. Furthermore, geopolymer has several advantages over traditional cement-based materials, such as higher initial mechanical strength, low drying shrinkage, high fire resistance, shorter curing time, higher resistance to acid attack [13–16]. Moreover geopolymer concrete is more resistant to chloride penetration because of its reduced overall permeability compared to Portland concrete [17].

However, the incorporation of MPCM in the geopolymer can be a solution to decrease the environmental impacts on two major phases of the building life cycle, which are the building operation phase (energy use to improve thermal comfort) and the cement production phase.

Shadnia et al. [18] constructed three small cells of activated fly ash geopolymer mortars. Among these three cells, two contain MPCM. Measurements of their internal temperature showed a reduction of 4.5 and 5.5°C for the two MPCM geopolymer cells compared to the reference cell. Cao et al. [5] numerically investigated the influence of different conditions on the energy efficiency of a wall constructed from geopolymer-MPCM concrete using the finite difference method. With the addition of 5.2% MPCM, there was a reduction in the interior wall temperature of approximately 3°C and a reduction in energy consumption of 25% to maintain the interior temperature at 23°C.

97 In contrast, to date, and based on all current research, most studies show that MPCM exhibits a
98 negative effect on the mechanical, physical and thermal conductivity performance of the cement
99 and geopolymer matrix [7,18–20].

100 Cao et al. [7] studied the effect of MPCM addition on the compressive strengths of Portland cement-
101 based concrete and geopolymer-based concrete. Their results show that the presence of MPCM
102 increased the heat capacity of both types of concrete studied up to the value of 1500 (J/kg ° C), but
103 the compressive strengths were reduced by about 42 and 51%. The same observations were reported
104 by Shadnia et al. [18] that cited a decrease in compressive strength of up to 25%. The study by Cao
105 et al. [21] showed that the decrease in mechanical performance is related to the increase in open
106 porosity when the concentrations of MPCM increase in the fly ash geopolymer concrete matrix.

107 Disadvantages of incorporating MPCM into the cement matrix include the rate of decrease in the
108 thermal conductivity of the total cement matrix [22]. Recall that in the case of a material not
109 containing MPCM, its thermal insulation performance is related to its low conductivity, which will
110 delay the penetration of heat into the building. Nevertheless, in the case of a material containing
111 MPCM, the decrease in its thermal conductivity will disrupt the latent heat of MPCM to complete
112 their charge-discharge cycle due to the low heat flux transmitted. This is a problem in this field and
113 has been highlighted by several researchers [23–25]. The effect of reducing thermal conductivity
114 after the addition of MPCM is similar to its effect on increasing porosity (porosity caused by the
115 presence of MPCM in the cement matrix) [22,23]. Several researchers have attempted to improve
116 the thermal conductivity of pure PCM (without capsules) after their incorporation into a cement
117 matrix by using some carbon-based or metal-based materials that have high thermal conductivity
118 [26–29]. Nevertheless, unfortunately, few studies have been conducted to improve the thermal
119 conductivity of a cement or geopolymer matrix after the incorporation of MPCM.

120 The scientific question of this study is how to overcome the negative effects of incorporating MPCM
121 into the geopolymer matrix to improve the mechanical and thermal performances of this new
122 material.

123 Concerning the use of geopolymer, we note that the main gel produced in the geopolymerization
124 process is in the form of a gel called sodium alumina silicate hydrate (NASH), resulting from the
125 activation of alumina and silica found in metakaolin or fly ash [30]. This gel is the result of the
126 chemical reaction between Na_2O-AL_2O_3-SiO_2-H_2O.

127 In recent years, several researchers have shown that it is possible to have in a single geopolymer
128 matrix another hydration gel in addition to the geopolymer gel itself. This gel can be obtained in a
129 matrix that is rich in calcium, silica and alumina to produce calcium alumina silicate hydrate
130 (CASH), and it is obtained from the chemical reaction between Na_2O-CaO-Al_2O_3-SiO_2-H_2O [31–
131 34]. The CASH gel results from the activation of blast furnace slag [35]. The use of calcium-rich
132 blast furnace slag with the inclusion of a small amount of silica (SiO_2) and alumina (Al_2O_3) rich
133 metakaolin (MK) contributes to a better workability and a structure mainly composed of the
134 coexisting gels mentioned above. This coexistence of gels, once obtained, improves the mechanical
135 performance and durability of the geopolymer [34].

136 However, most of the research that has been carried out on the geopolymer-MPCM is focused on a
137 geopolymer based on a unique base material such as GBFS, fly ash (FA), MK, etc. In addition, there
138 are few studies on combining two primary materials rich in calcium, alumina, and silica at the same
139 time, and no studies have investigated the inclusion of MK into a GBFS-based matrix containing
140 MPCM.

141 The aim of this study is to investigate the feasibility of developing the coexistence of CASH and
142 NASH gels in geopolymer-MPCM mortars to overcome the negative effects of MPCM
143 incorporation on the mechanical and thermal performance of these mortars. This coexistence of gels
144 will be achieved by adding three percentages of MK inclusion (0, 10 and 20%) in a GBFS-based
145 mortar. The geopolymer-MPCM mortars were also compared to Portland-MPCM cement-based
146 reference mortars.

147 Several characterizations of two types of mortar are carried out in this study, such as workability,
148 microstructure properties (SEM, EDS and XRD), water porosity, mechanical properties

149 (compressive strength, dynamic Young's modulus resistance) and thermal properties (thermal
150 conductivity, the specific heat capacity).

151 **2. Materials and experiments design**

152 **2.1. Materials**

153 The MPCM studied here is considered in the form of white spherical microcapsules marketed by the
154 laboratory Microteck-United States. Its technical name is Nextek 28 D. The microcapsule consists
155 of two parts, a polymer wall and the core material (paraffin). Its composition is ≥ 97% paraffin
156 powder. The polymer is a urea polymer, cross-linked with a modified low molecular weight
157 polyethylene. MPCM possesses a melting temperature between 26 and 28°C and a heat capacity
158 between 180 and 190 (J/g).

159 The density was measured by the pycnometer method according to NF T 20-053 and is equal to 0.84
160 g/cm^3, almost equal to the density of MPCM in the literature [7,18]. Its thermal conductivity was
161 measured with the Hot Disk 1500 device (the measurement procedure will be explained in the
162 following sections). It is equal to 0.2 W/mK. This value is the same as that found in the literature
163 [25]. MPCM grains range in size from 6.19 to 38.22 μm.

164 The GBFS was delivered by the company ECOCEM in France while the MK was provided by the
165 company KENZAI (ecological materials) in France. The cement used is CEM II (32.5). The
166 chemical compositions and physical properties of cement II, GGBS and MK are presented in Table1.

167 Table 1. Chemical composition and physical properties of CEM II, GBFS and MK.

Chemical composition (%)	**CEM II**	**GBFS**	**MK**
SiO_2	7,47	37,3	55
Al_2O_3	2,18	10,7	41
Fe_2O_3	2,84	0,2	1,2
CaO	69,02	43,0	0,1

MgO	-	6,5	0,2
TiO_2	-	0,7	0,4
$(Na_2O + K_2O)eq$	-	0,8	1,8
Specific gravity	3.03	2.90	2.40
Blaine specific surface area (m^2/g)	0.37	0.445	17
average grain size (μm)	8.47	13.25	7.13

168

169 According to Table 1, GBFS is composed of a sum of 48% SiO_2 and Al_2O_3 and a high content of
170 42.3% CaO while metakaolin MK is rich in SiO_2 and Al_2O_3 with a sum of 96%.

171 The mineralogical structure is shown by X-ray diffraction (XRD) in Figure 1. MK shows a sharp
172 crystalline peak at 32°, which is attributed to the presence of amorphous quartz structure (SiO_2) and
173 mullite crystalline phases ($Al_6Si_2O_{13}$). GBFS is composed mainly of an amorphous phase.

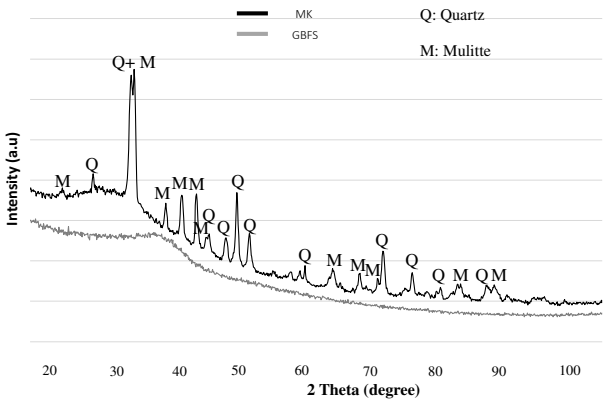

174

175 Figure 1. XRD patterns of MK and GBFS.

176 Figure 2 shows the particle size distribution of GBFS, MK, CEM II and MPCM, which was determined
177 using a laser granulometer type Cilas 1190. The measurements were performed using the wet method.
178 Indeed, we had doubts about the fact that water would not disperse MK particles, but the results of the
179 measurements are close to the results quoted in the study of Kamath et al. [35].

It is also noted that MK has finer particles than GBFS with an average particle size that is equal to 7.13 µm while the average particle size of GBFS and cement is equal to 13.25 µm and 8.47 µm. On the other hand, their specific surface areas are equal to 17; 0.44; and 0.37 m^2/g.

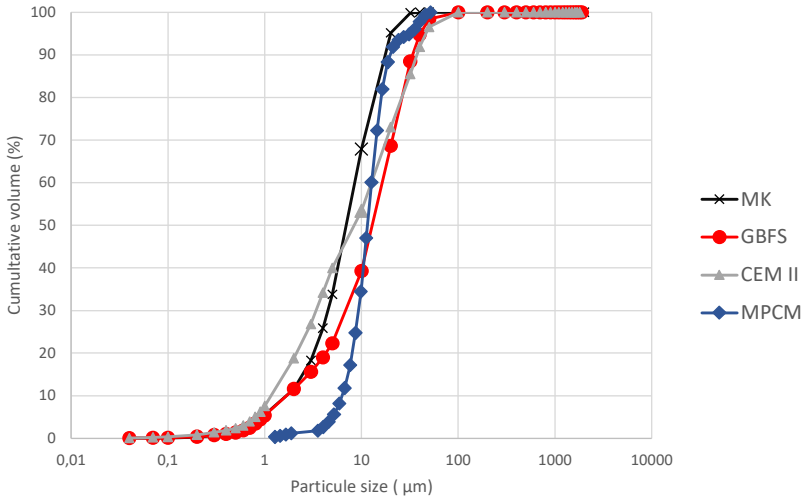

Figure 2. Particle size distribution of MK, GBFS, CEM II and MPCM.

The activation solution is a mixture of sodium silicate and sodium hydroxide. According to the supplier, the composition by mass of the sodium silicate is 27.53% SiO_2, 11.47% Na_2O and 61% H_2O. Sodium hydroxide NaOH is a caustic soda of 98% purity. The two solutions were provided by the company E2EM in France.

A standardized sand (CEN NF 196-1). This type of sand is generally used for laboratory tests. The supplier is the same as for two alkaline solutions. The purpose of using standardized sand is to eliminate the secondary effects on the binder of unfavorable impurities that natural sand may contain.

2.2. Mixing method and curing condition

Twelve formulations were investigated in this study; three were based on standardized mortar, and nine were based on geopolymer mortar. The water/binder ratio of 0.5 and the sand/binder ratio of 3 have been fixed for the two types of mortars, knowing that the equivalent binder for geopolymer (equivalent to cement) is considered as the total of GBFS, MK, and alkaline solution (solid part). For this, the mass

198 ratio (GBFS+MK)/SA was set to 3, SA corresponding to the solid part of the alkaline solution. These
199 choices are recommended by the study of Hasnaoui et al [14].
200 MK will replace part of the GBFS in the geopolymer matrix with three substitution rates (0, 10 and
201 20%). Bernal et al. [34] cited that increased MK content resulted in significant reductions in compressive
202 strength, due to the incomplete reaction of MK in the activation solution used. In fact, the optimal
203 parameters were determined in this study to provide a high alkalinity of the activation solution to get
204 good reactivity of the MK. Regarding this observation, a mass ratio of 2.5 between sodium silicate (SS)
205 and sodium hydroxide (SS/NaOH) was set according to the study of Bernal et al. [34].
206 The sodium hydroxide solution was prepared with a concentration of 12M and mixed with the sodium
207 silicate and allowed to cool for 24 hours before the mixing procedure.

208 A high concentration of NaOH (above 14M) can disrupt the dissolution of calcium in the matrix [36],
209 resulting in an absence of CASH gel, while a low concentration of NaOH does not allow the dissolution
210 of silica and aluminum in GBFS and MK, while the latter require sufficient Na^+ to be dissolved. Huseien
211 et al. [37] carried out a study on the effect of NaOH concentration in a geopolymer matrix. They
212 indicated that the mechanical properties and microstructures of the geopolymer were improved with a
213 concentration of 12M as chosen in this study.

214 Regarding MPCM, three concentrations were chosen of MPCM in the two types of mortar (cement-
215 based and geopolymer) such as 0; 5 and 10. The method chosen for the incorporation of MPCM in the
216 geopolymer is the method of replacement of sand by MPCM. This method is the most used in this field
217 and, according to the study by Pilehvar et al. [38], its use allows the least reduction of the mechanical
218 performance.

219 Table 2 illustrates the mixing proportions in kg/m^3. The first three formulations are based on
220 standardized cement mortar while the last nine are based on geopolymer.

221 The quantity of water in the two alkaline solutions is considered to have a water/binder ratio equal to
222 0.5.

223 Table 2. Formulations of cement II mortars and geopolymer mortars (kg/m^3)**.**

224

225

226

Mixtures proportions (kg/m^3)									
Sample	Cement	GGBS	MK	Sand	MPCM	Na_2SiO_3	NaOH	MGP water	MCII water
$MCII_{0/0/0}$	585,9	-	-	1757,8	-	-	-	-	293,0
$MCII_{0/0/5}$	585,9	-	-	1673,8	28,4	-	-	-	293,0
$MCII_{0/0/10}$	585,9	-	-	1582,0	56,8	-	-	-	293,0
$MGP_{100/0/0}$	-	439,5	-	1757,8	-	267,9	127,7	42,6	-
$MGP_{100/0/5}$	-	439,5	-	1673,8	28,4	267,9	127,7	42,6	-
$MGP_{100/0/10}$	-	439,5	-	1582,0	56,8	267,9	127,7	42,6	-
$MGP_{90/10/0}$	-	395,5	43,9	1757,8	-	267,9	127,7	42,6	-
$MGP_{90/10/5}$	-	395,5	43,9	1673,8	28,4	267,9	127,7	42,6	-
$MGP_{90/10/10}$	-	395,5	43,9	1582,0	56,8	267,9	127,7	42,6	-
$MGP_{80/20/0}$	-	351,6	87,9	1757,8	-	267,9	127,7	42,6	-
$MGP_{80/20/5}$	-	351,6	87,9	1673,8	28,4	267,9	127,7	42,6	-
$MGP_{80/20/10}$	-	351,6	87,9	1582,0	56,8	267,9	127,7	42,6	-

227

228 The standard NF 196-1 [39] was followed for the fabrication of standardized cement mortars, which
229 were chosen as a reference for comparison with geopolymer-based mortars. However, regarding the
230 mixing of geopoloymers, GBFS and MK were mixed with alkaline solution and water for 90 seconds to
231 produce a homogeneous paste [19,20]. The mixing was followed by the addition of sand and mixed for
232 5 minutes and finally MPCM was added and mixed for 2 minutes.
233 The idea of increasing the mixing time is recommended by Ahmari et al. [40] and is intended to allow
234 the efficient dissolution of silica, alumina, and calcium (Ca) in the alkaline solution. After the mixing

procedures, standardized cement mortars and geopolymers were used for the measurement of workability. After this step, the casting is done in specimens of 40 × 40 × 160 mm^3 and vibrated using an impact table and are stored in an air-conditioned room (temperature 20 ± 1° C and relative humidity 50 ± 5%)) for 48 hours before demolding. All samples except the standardized cement mortars (water conservation) were covered with plastic films.

2.3. Experimental methods

In this research, all the experiments tests were carried out at room temperature, i.e., between 19 °C and 21 °C, excepted the thermal properties (see dedicated item). All the tests, including age of mortars, are listed in Figure 3. The samples used have the same dimensions (40 × 40 × 160 mm^3) for mechanical tests, water porosity and thermal properties determination.

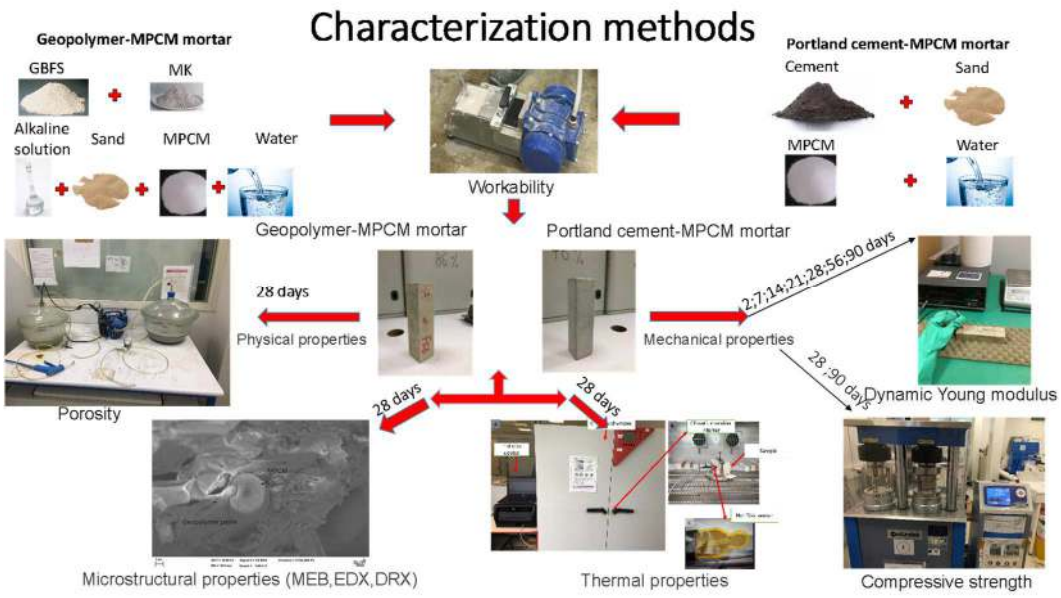

Figure 3. Characterization methods

The workability test was carried out directly after mixing according to standard NF P18-452 [41] using a workability meter. The test consists in measuring the flow time of mortars under the effect of the vibration caused by the vibrator. The water porosity was determined according to the NF P 18-459 standard [42].

Morphological analyses were performed using a ZEISS ЄVO®4 scanning electron microscope (SEM) combined with a BRUKER markeer energy dispersive X-ray spectroscopy (EDS) analyzer. The analyses

were performed on fractured samples after 28 days of curing. Indeed, the geopolymer samples were placed in the oven at 60°C to limit hydration before the SEM analyses. XRD analysis was performed on samples ground to powder using a mortar pestle, then sieved using an 80 µm sieve after 28 days of curing. Hydration was then stopped using an acetone quench. Measurements were performed using a SEIFERT MZ VI E X-ray diffractometer with Co Kα radiation and a constant scanning speed in the range 2θ = 15°-115 °.

Compressive strengths were performed according to the NF EN 196-1 [40] standard. These tests were carried out on six samples to ensure good repeatability. Dynamic Young's modulus measurements were performed following the ASTM E 1876-01 standard [43] and using the Grindosonic apparatus. These measurements were performed on three samples of each formulation at 2, 7, 14, 21, 28, 56 and 90 days. The technique is based on pulse excitation of the vibrations. This modulus is calculated with the use of the equation 1 and by using the flexural frequency (f_f) obtained during the measurement with the dimensions and weight of the samples:

$$\mathrm{E} = 0.9465 \times \left(\frac{m \times f_f^2}{\mathrm{b}}\right) \times \left(\frac{L^3}{t^3}\right) \times T_1 \qquad (1)$$

With E, f_f, m, L, b, t represent the Young's modulus (Pa), flexural frequency (Hz), mass in (g), length in (mm), width in (mm) and thickness in (mm) of the sample. T_1 represents correction factor that accounts for the finite thickness of the bar, Poisson's ratio, and so forth.

One of the main objectives of this work is to evaluate the thermal properties of the materials studied here to determine their thermal performance so that they can be used in the future in a real application. In the research field, there are two techniques for measuring the thermal properties of a material; namely, the steady-state measurement technique and the non-steady-state (transient) measurement technique [44]. Transient measurements have attracted a great deal of research because of their speed and accuracy. Among these is the hot disk technique which uses the transient planar source technique (Hot Disk TPS). The advantage of this method is that it can measure the thermal properties of a wide range of materials and measure the thermal conductivity in the range of 0.005 to 500 W/m.K.

The Hot Disk method can measure three thermal properties at the same time, such as thermal conductivity, thermal diffusivity, and specific heat capacity, using the TPS sensor, which has two roles (heat transmitter and temperature measurement receiver) [45].

Nevertheless, thermal property measurements with the TPS Hot Disk are often performed in an environment where the temperature is ambient (between 20 and 22°C). This is not possible in our case due to the melting temperature of the MPCM used in this study (between 26 and 28°C). Given this constraint, the measurements were carried out in a climate controlled chamber with a temperature range between 15 and 40°C and a constant humidity of 50%. The climatic chamber used is the KBF 720 type. Its temperature ranges are between 0 and 70 ° C while the relative humidity ranges are between 10 and 80 %.

Figure 4 shows a picture of the climatic chamber and the hot disk device with the measurement samples.

Figure 4. Thermal measuring device, A: climatic chamber and hot diskt; B: interior view of the climatic chamber; C: the measuring sensor

The thermal conductivity is influenced by the moisture content of the measurement samples. Due to this influence, the measurements were carried out on samples dried at 60 °C until they had a constant mass. This drying method was recommended by Zhang et al. [46]. Thermal measurements are performed by placing the sensor on the upper surface of the sample, which is connected to a data acquisition unit as shown in Figure 4.

3. Results and discussion

3.1. Workability

Figure 5 shows the flow time of the different formulations studied. It should be noted that the main ratios [Water/Binder, (GBFS+ MK)/SA, SS/NaOH and NaOH concentration] that affect the workability of the geopolymer were fixed. The increase in the ratio (GBFS+ MK)/SA increases progressively the flow time, which means that the workability of geopolymer mortars decreases with the incorporation of raw materials (GBFS+ MK). This decrease is due to the high water demand of raw materials, especially metakaolin, which has a high specific surface [14]. On the other hand, increasing the SS/NaOH ratio and the concentration of NaOH increases the viscosity of the activation solution and thus reduces the flow of the mortar. This is due to the very high viscosity of sodium silicate and sodium hydroxide [47].

Then the only variables in this study are the MPCM in both types of mortar (cement-based and geopolymer) and the MK in the geopolymer mortar. Cement mortar without MPCM showed a flow time of about 7 seconds that is confirmed from the literature [14].

Furthermore, as the MPCM concentration increases, the flow time increases for both types of mortars, meaning that workability is reduced. This effect is attributed to the agglomeration of MPCM during mixing due to its small size. This causes a larger water adsorption surface compared to the sand surface. Indeed, MPCM traps water and prevents it from penetrating the matrix, which results in a decrease in workability. In fact, MCPM strongly affected cement mortars while it did not show significant effects on geopolymer mortars. This difference is explained by the very high workability of geopolymers compared to cement-based mortars. This is related to the difference in activation of aluminosilicate materials compared to cement-based materials, as confirmed by Muhammad et al. [48] and Deb et al. [49].

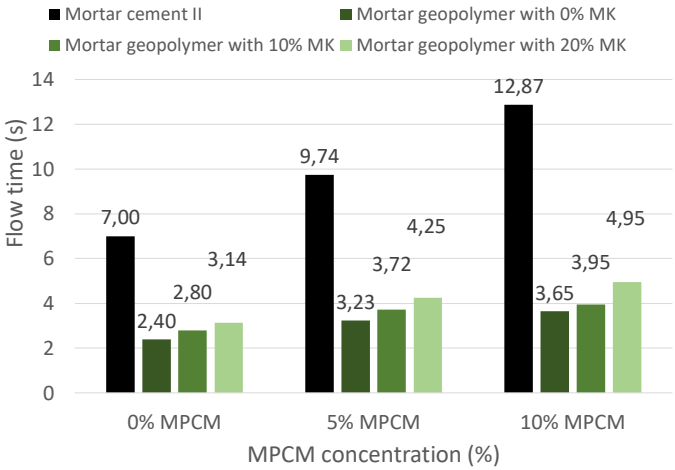

Figure 5. Workability of different formulations

It is further observed that there is a slight increase in the flow time in all the mortars of geopolymers with 10 and 20% MK. This increase is related to the water demand of MK due to its large specific surface area.

Based on the comparison with the flow time of cement-based mortars, geopolymer-MPCM mortars showed good workability using up to 10% MPCM and 20% MK where the maximum flow time is equal to 4.9 seconds that is lower than the flow time of Portland cement-based mortar (7 seconds).

3.2. Microstructural analysis

Morphological analyses were performed with SEM for the observation of the microstructure of the geopolymer samples and EDS for the analysis of the elemental composition. Figure 6 compares the fractured geopolymer samples $MGP_{100/0/0}$ (Figure 6.A) and $MGP_{80/20/0}$ (Figure 6.B).

The SEM observations clearly show the appearance of additional gels in the matrix with 20% MK (Figure 6.B), while this appearance of gels was not observed in the matrix with 0% MK. The EDS analyses showed the presence of the main elements Si, Al, Ca, Na, which shows the formation of CASH gel, the main component of the GBFS activation [35,50]. Indeed, the analyses also show a higher content of the main elements mentioned previously for the $MGP_{80/20/0}$ formulation compared to the $MGP_{100/0/0}$ formulation. The increase in Si, Al, Ca, Na confirms the presence of NASH in addition to CASH gel in

the $MGP_{80/20/0}$ formulation. According to Mijarsh et al. [30], the coexistence of these two gels results a single stable gel called (C, N)ASH.

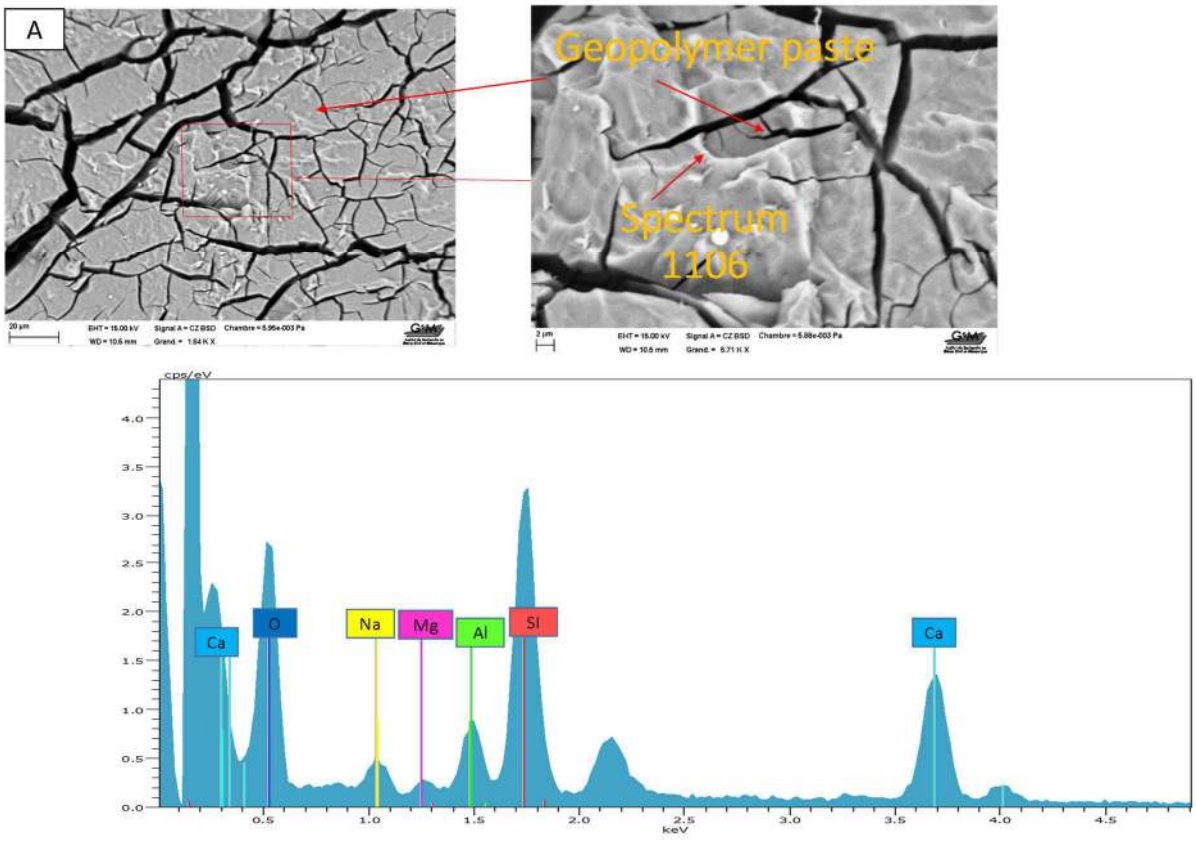

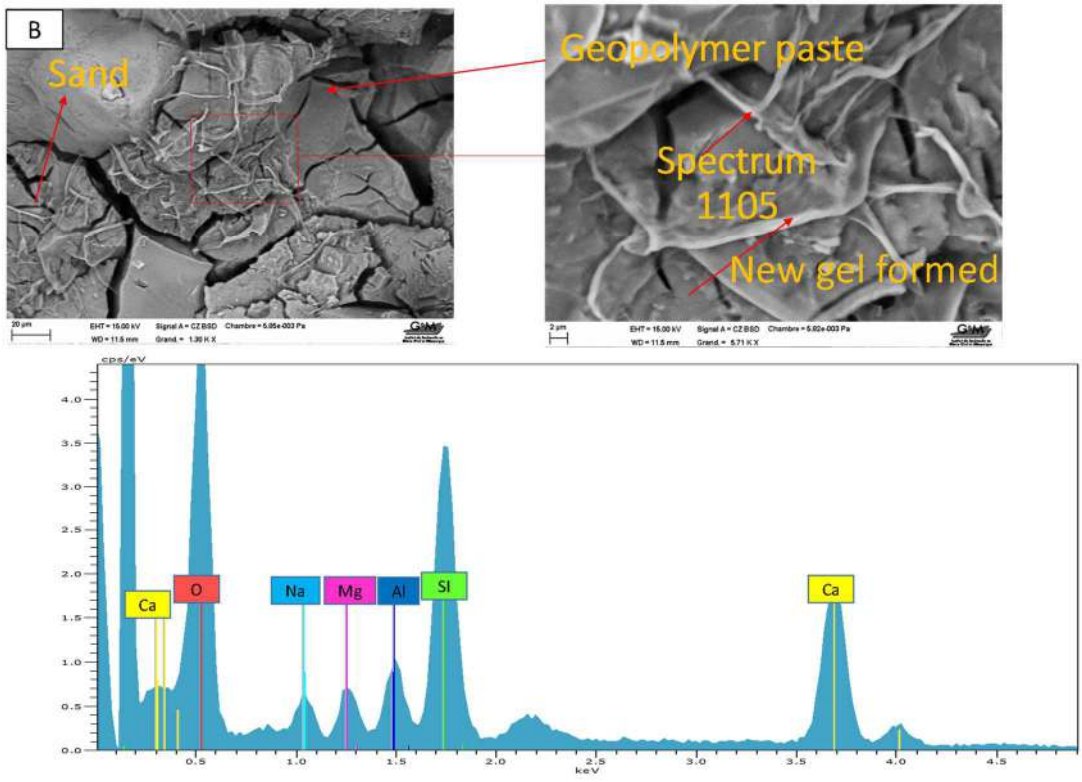

343

344 Figure 6. Microstructures of fractured samples at 28 days, A: $MGP_{100/0/0}$; B: $MGP_{80/20/0}$.

345 Table 3 compares the elemental compositions obtained by EDS of the geopolymer mortars $MGP_{100/0/0}$,
346 $MGP_{100/0/10}$, $MGP_{80/20/0}$, and $MGP_{80/20/10}$.

347 Table 3: Elemental compositions of $MGP_{100/0/0}$, $MGP_{100/0/10}$, $MGP_{80/20/0}$, $MGP_{80/20/10}$.

348

	Specimen			
Elemental compositions (%)	**$MGP_{100/0/0}$**	**$MGP_{80/20/0}$**	**$MGP_{100/0/10}$**	**$MGP_{80/20/10}$**
O	60,69	54,71	65,91	58,17
Si	14,68	18,16	14,32	20,97
Al	3,64	3,94	2,79	3,74
Ca	15,05	19,35	12,29	14,06
Na	3,31	3,20	3,66	2,25

Si/Al	4,03	4,60	5,13	5,60

Table 3 shows that the concentrations of silica, calcium and aluminum increased after the addition of 20% MK. The mass content of silica is equal to 14.68% in the case of $MGP_{100/0/0}$ while it increased to 18.16% with 20% MK ($MCP_{80/20/0}$). This content also increased from 14.32 to 20.97% in the geopolymer mortar which contains 20% MPCM after the inclusion of 20% MK. Indeed, the main precursors of MK activation are Si and Al, which may indicate that the high silica and alumina content of MK was well dissolved by alkaline activation to form Si-O-Si and Si-O-Al bonds. On the other hand, the increase in silica content increased the Si /Al ratio, confirming that the Si-O-Si bond was dominant over the Si-O-Al bond. The Si/Al ratio increased from 4.03 in the $MGP_{100/0/0}$ matrix to 4.60 in the $MGP_{80/20/0}$ matrix, and from 5.13 in $MGP_{100/0/10}$ to 5.6 in $MGP_{80/20/10}$. The increase of the Si/Al ratio improves the microstructure of the geopolymer, which results in an increase in its mechanical performance [30,51,52].

Moreover, it is also noted that the calcium content increased after the addition of MK, showing that the calcium reacted well to the addition of MK and that its dissolution is not disturbed by the presence of the 12M NaOH concentration. The increase in the calcium content increases the mechanical performance of the geopolymer, as it will be shown in section **3.5** [34,53,54].

In addition, the presence of CASH and NASH gel can be confirmed by the mass ratio values in percentages of Na/Si, Al/Si, Ca/Si. The Na/Si ratios are between 0.10 and 0.22 and Al/Si ratios are between 0.17 and 0.24. They are in the range of the study by Ibrahim et al. [51] from which they confirmed the appearance of these gels. On the other hand, the Ca/Si ratios are between 1.02 and 1.06, which are higher than their ratios. This difference is due to the use of up to 80% GBFS in this study with high calcium content.

3.3. X-ray diffraction analysis

Figure 7 shows the XRD analyses performed on the powders of samples $MGP_{100/0/0}$, $MGP_{90/10/0}$ and $MGP_{80/20/0}$ at 28 days. From a global point of view, it appears that all the samples show crystalline phases. Around the 35° peak, the presence of hillebrandite of chemical formula $Ca_2\ SiO_3\ (OH)_2$ is observed in

all samples. Indeed, hillebrandite belongs to the CSH family of gels; Mijarsh et al. [30] explained that with the presence of aluminum, the main composition of CSH turns into CASH gel. These results were observed in EDS in the previous section (**3.2**) and are due to the use of up to 80% GBFS which leads to the creation of CASH gel in general.

Several researchers have confirmed the presence of hillebrandite around this peak at 35° [30,55,56]. On the other hand, Mijarsh et al. [30] have noted that hillebrandite serves the improvement of the mechanical performance of the geopolymer. These results are in good agreement with the mechanical performance results in Section **3.5.1**.

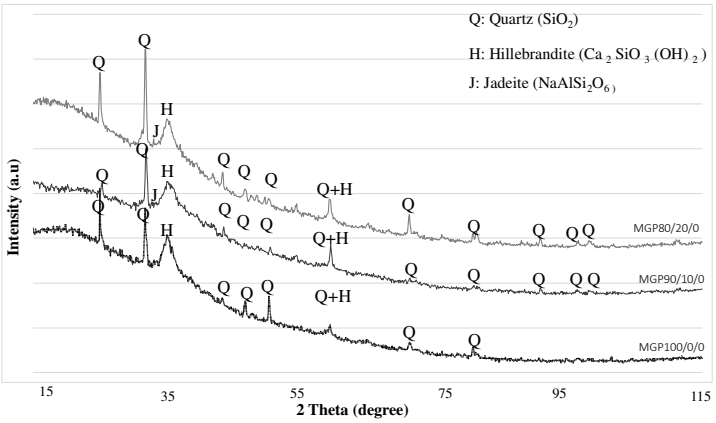

Figure 7. X-ray diffraction of samples $MGP_{100/0/0}$; $MGP_{90/10/0}$; $MGP_{80/20/0}$) at 28 days.

After MK inclusion, the peak of jadeite ($NaAlSi_2O_6$) increased around 33°. Jadeite is a member of the NASH family (the main gel for MK activation) [30]. It has a crystal structure with tetrahedral Si coordinated in single chains and Al and Na in octahedral coordination [30,57]. The presence of hillebrandite and jadeite in a single matrix confirms the coexistence of NASH and CASH gel and results also in a high mechanical strength [51,55]. According to Ibrahim et al. [51], the CASH and NASH gel renders the microstructure very compact and dense and this serves to improve the mechanical strength. Indeed, this can be explained by the dissolution of silica, alumina, and calcium, which serve to fill the small pores in the geopolymer matrix [50]. EDS analysis also showed that the silica, alumina, and calcium contents were increased after the addition of MK.

On the other hand, around the 60° peak, the intensity of the hillebrandite plus quartz (SiO_2) peak was increased. This clustering may be related to the participation of calcium after the inclusion of MK in the formation of the CASH gel with the presence of the NASH gel. The EDS confirmed the same observations where the calcium content was increased after the inclusion of MK. Regarding this observation, it is not possible to confirm these results because the samples used are in the form of mortars (presence of sand). Quartz is therefore the main element of the sand.

3.4. Water porosity and apparent density

Figure 8 shows the water porosity results as well as the density of the studied samples. It indicates that the cement-based mortar without MPCM presents a porosity of 17.90%. This value is approximately similar to that reported in several studies that have investigated porosity for standardized cement mortars [14,58].

It is noted that the porosity values of geopolymer mortars without MPCM are lower than those of cement-based mortars. This difference may be related to the difference in workability between the two types of mortars in section **3.1**. Yang et al. [59] mentioned similar observations and cited that the improvement of the workability of geopolymer reduces its porosity.

In addition, the increase in MPCM concentration caused an increase in porosity and a decrease in density of all the samples studied. The decrease in density may be caused by the difference in density between the sand (2.6 g/cm^3) and the MPCM (0.84 g/cm^3). Furthermore, the increase in porosity may be due to the MPCM not filling the matrix cavities due to their agglomeration surface area being larger than that of the sand. This agglomeration surface serves to adsorb a small amount of the binder paste, while this can produce voids during mixing and increase porosity.

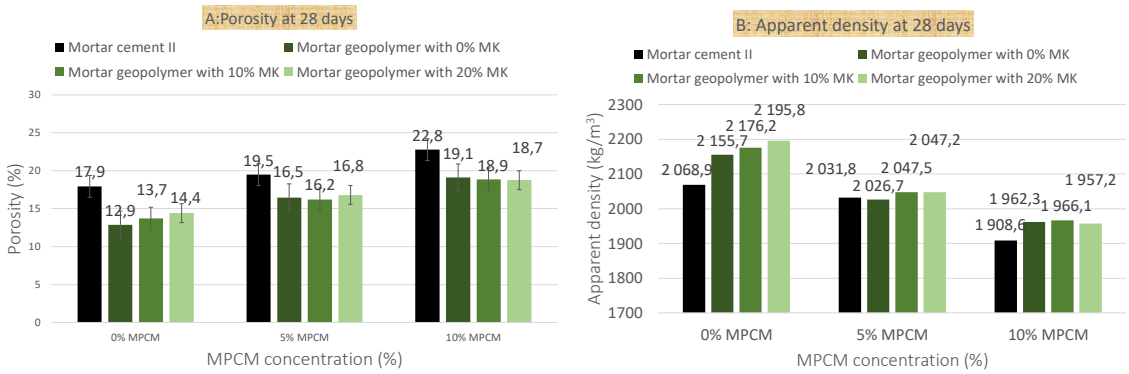

Figure 8. Water porosity and apparent density at 28 days.

However, the addition of MK shows no effect on porosity, showing that MPCM exerts a major effect on controlling the porosity of the geopolymer samples studied here. In contrast to the porosity results, the density was improved after the addition of MK in the samples without MPCM. This improvement was due to the high reactivity of MK compared to GBFS, which promoted the good dissolution of silica and aluminum to form new NASH and CASH gels in the matrix, as shown in Sections **3.2** and **3.3**.

3.5. Mechanical properties

3.5.1. Compressive strength

Figure 9 shows the results of the compressive strength at 28 and 90 days. Globally, it should be noted that there is no significant difference between the compressive strength between 28 and 90 days for geopolymer mortars, contrary to cement-based mortars, which show an increase in their compressive strength between 28 and 90 days. Geopolymer is considered as a material that can gain most of its mechanical strength in the first few days of curing due to its strong chemical bonding, unlike cement-based materials.

Bernal et al. [34] found that there is no difference in the compressive strength between 28 and 90 days for geopolymer without the addition of metakaolin (100% GBFS), while Bai et al. [60] pointed out that the increase in the GBFS rate serves to accelerate the development of the mechanical strength of the geopolymer. This may explain why there is no great difference between the 28- and 90-day time frames in this study.

The compressive strength of geopolymer mortars (with and without MPCM) is higher than the compressive strength of cement-based mortars. This may be related to the optimal formulation ratios that have been set according to the literature [14,34,37] and that have contributed to the improvement of geopolymerization.

The compressive strength of cement-based mortars decreases as the rate of MPCM incorporation increases. After 28 days, the compressive strength decreased from 32.6 to 29.2 MPA with 5% MPCM and then to 25.6 MPA with 10% MPCM. The effect is remarkably similar after 90 days. In the case of geopolymer-based mortars containing 0% MK, the same results are obtained. The compressive strength value in this case decreased from 69.9 to 50 MPA with 5% MPCM and reached 40.8 MPA with 10% MPCM after 28 days. Therefore, the rate of reduction of mechanical performance of geopolymer mortars with 10 and 20% MK is less compared to geopolymer mortars without MK.

The compressive strength value for the 10% MK geopolymer mortar is reduced from 69.08 to 60.12 with 5% MPCM, and then it is reduced to 47.9 MPA with 10% MPCM, while for the 20% MK geopolymer mortar, the value is reduced from 78.5 to 58.9 until it reaches a value of 49.5 MPA.

This reduction in compressive strength is caused by the effect of replacing MPCM with sand. Recall that MPCM has replaced a certain volume percentage of sand in the matrix. Therefore, MPCM has low stiffness and mechanical strength compared to sand and can easily break under compressive force [7,18,23]. Furthermore, the increase in matrix porosity after MPCM incorporation is one of the causes of the reduction in mechanical strength as observed in the results detailed in the section. **3.4**.

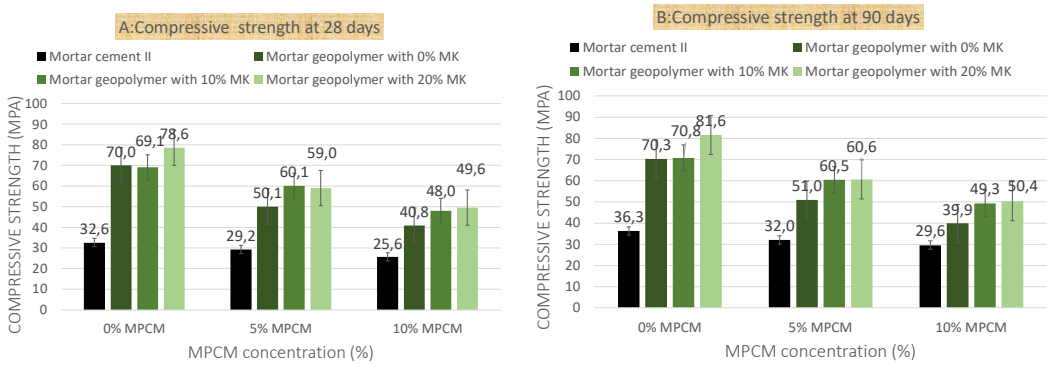

Figure 9. Compressive strength; A: 28 days; B: 90 days.

In addition, it can be observed that the geopolymer mortars with 0% MK showed a high mechanical strength. This increase is caused by the high activator content and is due to the high Si/Al ratio [61]. The presence of this high ratio in this study can be explained by the good dissolution of silica ions and alumina of the GBFS due to the high PH of the solution, which results in a gel with high mechanical performance [34].

Moreover, the addition of 10% MK in geopolymer mortars with MPCM concentrations (5 and 10%) led to an increase in compressive strength at 28 days. The value increased from 50.06 to 60.12 MPA (geopolymer mortar with 5% MPCM) and from 40.8 to 47.9 MPA (geopolymer mortar with 10% MPCM) compared to the mortar without MK. The same effect of the addition of MK on the increase of compressive strengths is observed also at 90 days. On the contrary, the addition of 10% MK did not show any improvement in the compressive strength for geopolymer mortars without MPCM. About this observation, the CASH and NASH gels created after the addition of MK showed a significant effect on the mortars that have both concentrations of MPCM. Indeed, these mortars showed a high porosity, while CASH and NASH gels are generally used to fill small pores [51]. This observation may be the reason for the improved compressive strength.

In the case of the addition of 20% MK, the compressive strength is almost the same in the case of 10% MK compared to the geopolymers with 5 and 10% MPCM, but for the geopolymers without MPCM, the strength was increased from 69.9 to 78.5 MPA at 28 days and it reaches 81.6 MPA at 90 days. This effect of increased compressive strength can be explained by the small particle size and large specific surface area of MK compared to GBFS, which allow for accelerated reactivity [31,62] on the one hand, and the large amount of Al_2O_3 and SiO_2 in MK. These two effects led to an improvement in geopolymerization by producing sodium aluminosilicate hydrate (NASH) gel and calcium silicate hydrate (CASH) gel in addition to the CASH produced by the activation of GBFS, which are rich in calcium [34].

In a matrix that contains both NASH and CASH, the geopolymerization process proceeds through the following steps:

1. The NASH gel is formed in a system containing Na_2O-Al_2O3-SiO_2-H_2O and starts with the dissolution and hydrolysis of the silica and alumina of the aluminosilicate material to form Si-OH and Al-OH bonds and continues with a condensation. The hydrolysis of Si and Al is presented in the following equations (2), (3), (4) [30,63]:

$$Al_2O_3 + 3H_2O + 2OH^- \rightarrow 2[Al(OH)_4]^- \quad (2)$$

$$SiO_2 + H_2O + OH^- \rightarrow [SiO(OH)_3]^- \quad (3)$$

$$SiO_2 + 2OH^- \rightarrow [SiO_2(OH)_2]^{2-} \quad (4)$$

However, the activator content (Na and Si concentrations) has a very important role in the condensation process, which strongly influences the properties of the geopolymer [30]. The use of a high activator content as in this study favored the condensation to form oligomeric silicates, which generate rigid polymeric 3D structures [poly (sialate-siloxo) and poly (sialate-disiloxo)] with Si/Al ratios greater than 2. Otherwise, the use of a low concentration of activator results in poly (sialate) polymer structures with Si/Al ratio equal to 1 and accompanied by low mechanical strength [30].

The EDS analyses in section **3.2** confirm that the Si/Al ratio is higher than 2, which explains the better mechanical strengths found in this study.

2. The CASH gel is formed in a system containing CaO-Na_2O-Al_2O_3-SiO_2 -H_2O. Calcium influences in a very important way the acceleration of the hardening and the improvement of the mechanical performances of the geopolymer because of its additional nucleation sites [30,34]. This may be one of the reasons for the improvement in mechanical performance, and the EDS analysis shows that the calcium content was increased after the addition of MK. The increase in this content confirms that it was indeed involved in the formation of both gels. These are two mechanisms cited by other researchers [30,40,64] to explain how calcium is involved in the geopolymer system. The first states that Ca^{2+} acts as a charge balancer and this allows it to be integrated into the geopolymer network. The second mechanism indicates that Ca is a contributing element to the formation of a CASH gel which has the possibility to coexist with the NASH geopolymer gel as explained above.

508 The reason for the increase in mechanical performance may be that the CASH and NASH gels
509 caused by MK activation filled the pores caused by MPCM, which was not observed in the
510 geopolymer with 0% MK.

511 The other reason for the improved mechanical performance may be related to the strong chemical
512 structure of the geopolymer after the addition of MK. This effect is confirmed by EDS, which shows
513 that the silica content increased after the addition of MK, which increased the Si/Al ratio. With the
514 increase in Si content, more silicate species are available for condensation and reaction between
515 them, resulting in more oligomeric silicates and they become dominant [62]. Researchers have
516 shown that oligomeric silicates of Si-O-Si bond are stronger than those of Si-O-Al and Al-O-Al.
517 This can explain the increase in compressive strength of geopolymer mortars after the addition of
518 MK, on the other hand [14,65].

519 **3.5.2. Dynamic Young's modulus**

520 The results of the Young's modulus at different times (2, 7, 14, 21, 28, 56 and 90 days) are shown
521 in figure 10. First, it can be noticed that this modulus develops with the curing time for both types
522 of mortar. This observation is an indication that the hydration of the cement and the
523 geopolymerization remain continuous during this time. Comparing the hydration time for cement
524 mortar and geopolymer, it is observed that the values of this modulus continue to increase for cement
525 mortars up to 90 days, while for geopolymer their values have been stabilized from the 14th day.
526 This is due to the very rapid acceleration of the mechanical strength of these materials compared to
527 cement-based materials [60].

528 Contrary to the compressive strength values, the Young's modulus values of the cement-based
529 mortar are higher than those of the geopolymer mortar. Although this effect has been granted
530 according to the literature [14,58,66], which cites that geopolymer possesses low rigidity, in contrast
531 the values of this modulus in this study are very close to those of standardized mortars with a
532 maximum value equal to 35.1 GPA at 90 days (geopolymer mortar with 20% MK without MPCM).

Figure 10 shows that the inclusion of MPCM decreased the Young's modulus for the two mortars (cement and geopolymer). These results are like the compressive strength results in the previous section (**3.5.1**).

The values of Young's modulus of cement-based mortar decreased from 35.7 GPA to 32.6 and 28.6 GPA with 5 and 10% MPCM at 28 days. This decrease after the incorporation of MPCM was accorded with the study of Šavija et al. [67]. Moreover, the same effects are observed in geopolymer mortars with 0% MK from which the values decreased from 34.0 to 27.7 and 19.8 GPA with 5 and 10% MPCM.

The reason for the decrease in Young's modulus is explained in section **3.5.1** of compressive strength. The Young's modulus depends on the strength of the material [68], so the inclusion of MPCM decreases the rigidity of the matrix due to its low rigidity compared to sand. The second reason may be due to the porosity caused by these materials, which decreases the flexural resonance frequency (f_f) while the latter is the main element that controls this modulus.

Figures 10.C and 10.D show that the MK inclusion rates improved the Young's modulus for all geopolymer samples. The addition of 10% MK increased the Young's modulus value of geopolymer mortars from 34.1 to 34.9 GPA (0% MPCM) and from 27.7 to 32.1 GPA (5% MPCM) and from 19.9 to 26.6 GPA (10% MPCM).

Similar remarks are reported in Figure 10.D (20% MK), which shows that the addition of 20% MK increased the Young's modulus values to 35.1, 29.9 and 26.4 GPA.

The optimum MK content is 10% for geopolymer-MPCM mortars, but for geopolymer mortars without MPCM, the optimum content is 20% MK. These results are in good agreement with the compressive strengths and can be explained by the pore filling effect caused by the activation of silica and alumina in the MK.

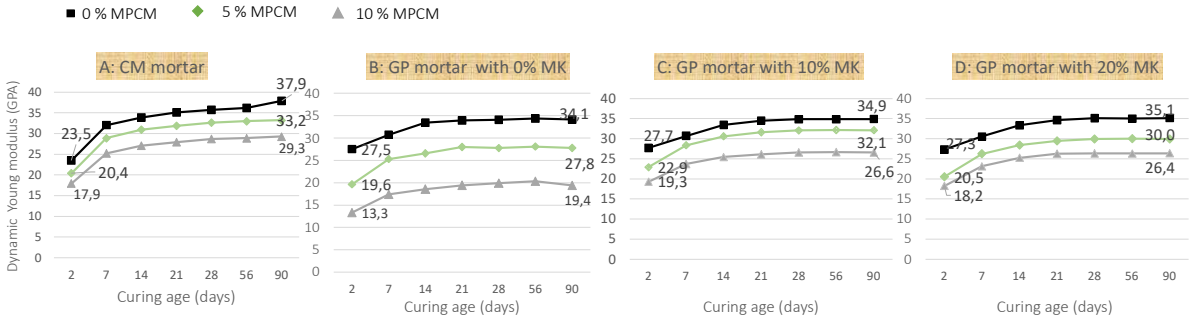

Figure 10. Young's modulus as a function of curing time, A: (cement-based mortar), B: (Geopolymer mortar with 0% MK); C: (Geopolymer mortar with 10% MK); D: (Geopolymer mortar with 20% MK).

Figure 11 represents a comparison of dynamic Young's modulus results on geopolymer mortars with other researchers who have used dynamic methods to evaluate the values of this modulus [14,69].

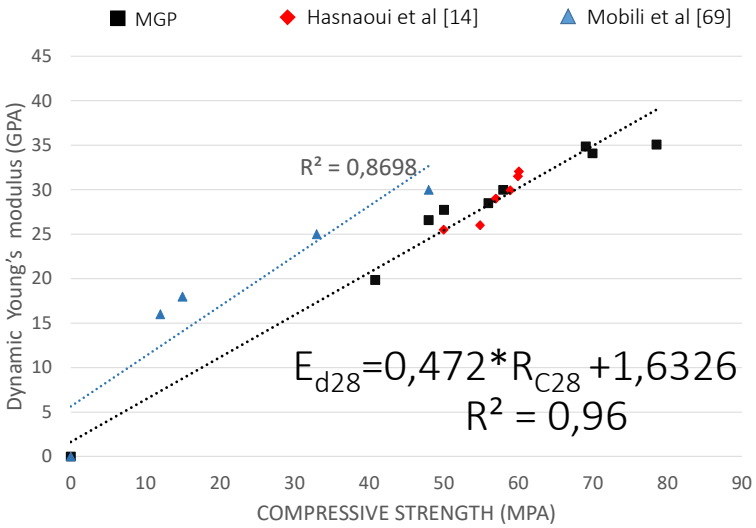

Figure 11. Correlation between dynamic Young's modulus and compressive strength at 28 days.

According to figure 11, there is a good correlation between this modulus and the compressive strength expressed by a linear variation with a correlation coefficient R2 = 0.96 for our geopolymer mortars and those of Hasnaoui et al. [14] and a linear correlation for the mortars of Mobili et al.

[69]. Indeed, Duxson et al. [65] indicated that the Young's modulus of the geopolymer is correlated with its compressive strength.

The results presented in this study are higher than the reference results mentioned. This is probably the consequence of the use of 80/20 GBFS and MK, in contrast to Hasnasoui et al. [14] who used 50/50 GBFS and MK, and the use of Mobili et al. [69] up to 100% fly ash. The CASH gel formed by GBFS activation is denser compared to the NASH gel and has a higher pore filling capacity [70,71], which may explain the better mechanical performance obtained in this study compared to the two references above.

3.6. Thermal properties

Figure 12 shows the thermal properties of two types of mortars at different measuring temperatures. These measurements were performed in a temperature range that is between 15 °C (MPCM in solid state) and 40°C (MPCM in liquid state). It can be clearly shown that the rate of increase of MPCM concentration caused a decrease in the thermal conductivity of two mortars (cement-based mortar and geopolymer-based mortar) independently of the measurement temperature. The reason for this decrease in the two cases can be explained by the two effects below:

- The first effect is attributed to the low thermal conductivity of MPCM (about 0.2 W/m.K), which replaced sand while the latter has a higher thermal conductivity. This effect was confirmed by the measurements that were carried out in the materials section (**2.1**).
- The second effect is the appearance of voids in the matrix after the incorporation of MPCM (see figure 8). These voids will transfer the heat flow from the state of conduction to the state of convection, resulting in a decrease in thermal conductivity.

However, the thermal conductivity in the solid state (measured at 15°C) of the two mortars with the two MPCM concentrations is higher compared to the thermal conductivity in the liquid state. This is confirmed by the study of Cui et al. [25] and Cao et al. [7] and due to the thermal conductivity of the solid state paraffin, which is generally higher than its thermal conductivity in the liquid state. Additionally, Sasaguchi et al. [72] have shown that the thermal conductivity of paraffin-type phase

change material (n-octadecane) in the solid state is equal to 0.358 W/mK while in the liquid state is equal to 0.148 W/mK.

Nevertheless, the MPCM did not show an improvement in the specific heat capacity of the cement mortars and that of the geopolymer without MK (figures 12 A and B).

This consequence can be related to the low thermal conductivity of the samples presented in figure 12 and due to the presence of more voids which appeared (figure 8 A). Indeed, these voids did not allow the ambient heat to transmit to the microcapsules to be stored on the one hand and can be related to the hot disk sensor which did not capture the latent heat stored by the MPCM on the other hand.

These results are not in agreement with the following references [9,18,73] which found an improvement in heat capacity with the use of the DSC method. When using the DSC method, the sample tested is in the form of a homogeneous powder with a mass of about 1-10 mg. Therefore, this method does not consider thermal conductivity, unlike the hot disk method used in this study.

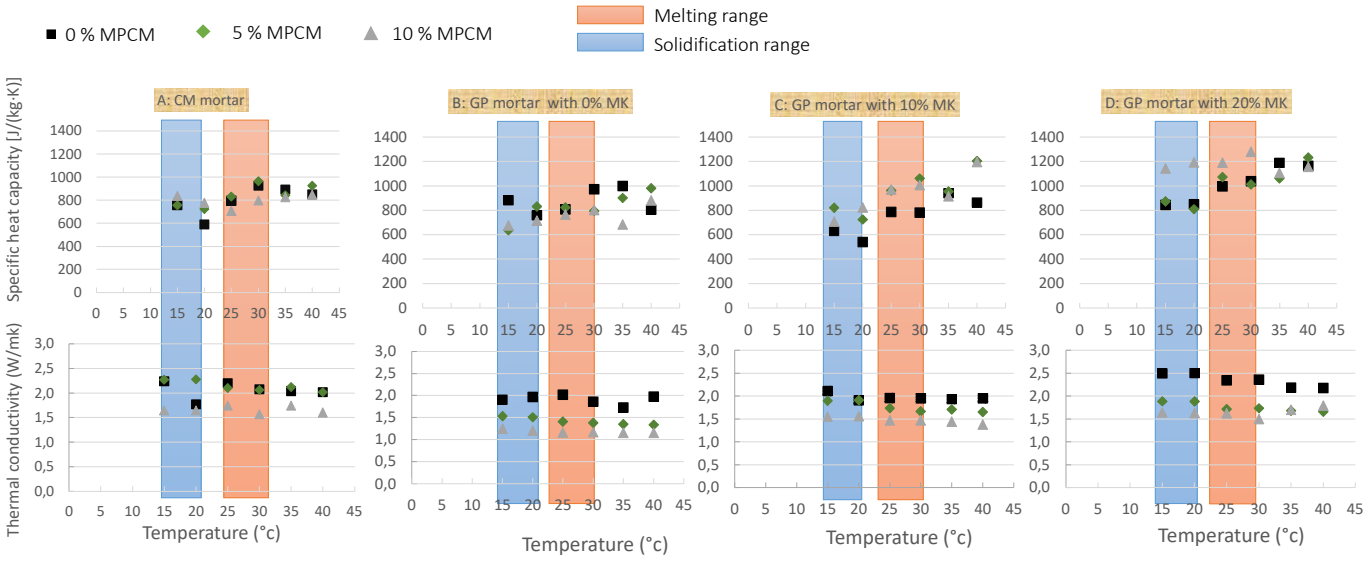

Figure 12. Thermal properties at 28 days; A: (cement-based mortar), B: (Geopolymer mortar with 0% MK); C: (Geopolymer mortar with 10% MK); D: (Geopolymer mortar with 20% MK).

In contrast to geopolymer mortars without MK, all samples with 10 and 20% MK showed the highest specific heat capacity at the melting point of MPCM (between 25 and 30°C) and at the solidification point (between 15 and 20°C). The highest value of specific heat capacity reached 1280.76 J/Kg.K at the melting range for $MGP_{80/20/10}$ (20% MK and 10% MPCM). This value is close to the one that is in the study of Cao et al. [7] who found a value of 1500 J/kg.K at the melting point of MPCM while they used up to 72 kg/m^3 of MPCM while in this study the concentration of MPCM is equal to 56.8 kg/m^3. The same improvements were accorded by Shadnia et al. [18], who found an improvement in specific heat capacity up to 1200, 33 J/kg.K. With this value of specific heat capacity, the conclusion of the study by Shadnia et al. [18] indicates that the internal temperature measurements of two cells constructed with geopolymer-MPCM mortar showed a reduction of 4.5 and 5.5 ° C compared to a reference cell that does not contain MPCM. In this case, the improvement of the specific heat capacity is related to the increase of the thermal conductivity.

Figure 13 is extracted from Figure 12. It shows the effect of the addition of MK on the thermal conductivity of geopolymer mortars in the solid state where the measurements are taken at 15°C. This point was chosen because the effect of adding MK on the thermal conductivity is roughly similar compared to the other measurement points.

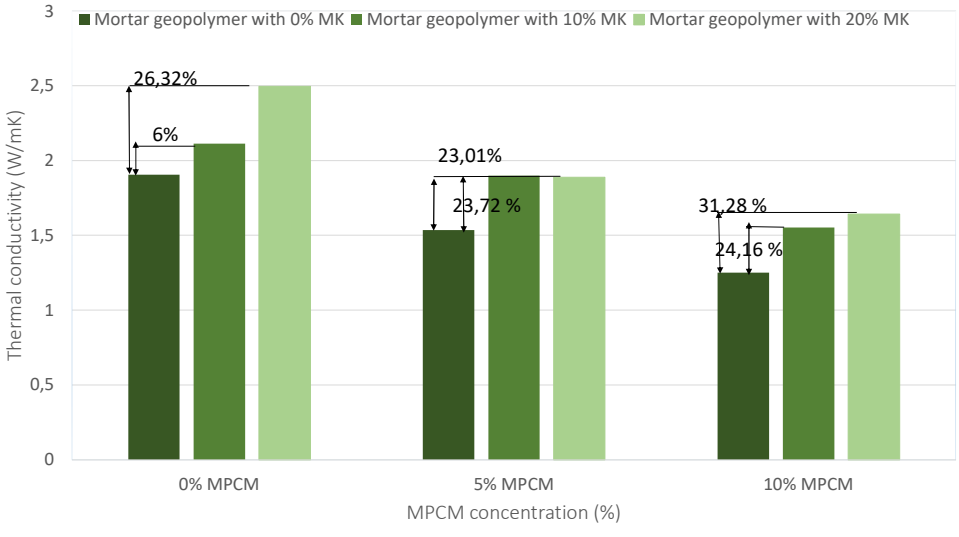

Figure 13. Thermal conductivity of geopolymer mortars at 15°C as a function of MPCM concentration before and after MK addition.

In Figure 13, it is clearly shown that the inclusion of two MK rates (10 and 20%) increased the thermal conductivity by 6 and 26.32% for the geopolymer mortar with 0% MPCM. This increase translates into an improvement in thermal conductivity of about 0.137 W/mK and 0.52 W/mK. On the other hand, an improvement in thermal conductivity of 23.01; 23.72; 24.16 and 24.16% is observed for geopolymer mortars with 5 and 10% MPCM. The increase of thermal conductivity after the inclusion of MK can be explained by the decrease of voids in the matrix due to the creation of gels in the geopolymer matrix, as several researchers have mentioned the advantage of the good reactivity of MK [14,34,53]. In addition, Ibrahim et al. [51] pointed out that the high Si content observed in the EDS leads to the filling of the pores of the studied matrix.

Figure 14 was obtained from the SEM for $MGP_{80/20/20}$ (20% MK and 20% MPCM). It shows a good cohesion of the geopolymer paste with the MPCM, which can explain the improvement of the thermal conductivity of the total matrix after the addition of MK and might be due to the increase of the thermal flux that was transmitted during the measurement.

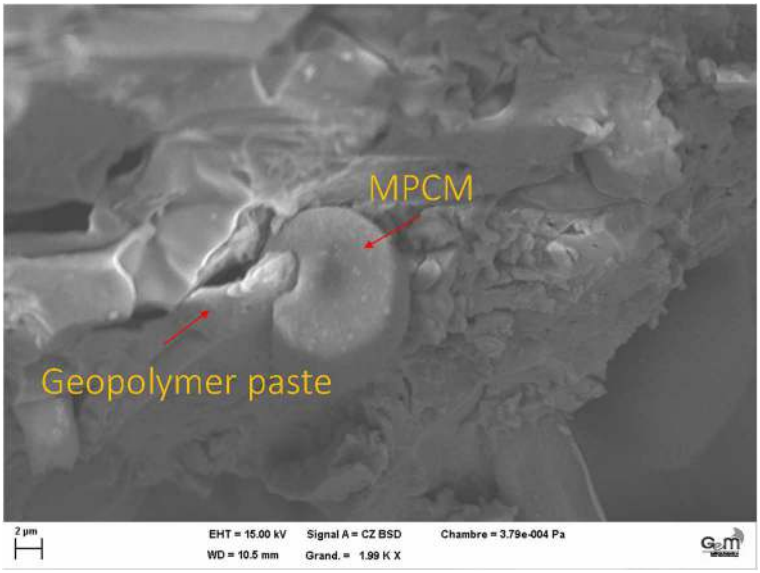

Figure 14. Cohesion of the geopolymer paste with MPCM.

XU et al. [74] added carbon nanotubes to a cement matrix to increase its thermal conductivity after incorporation of PCM (without capsule). They found an increase of about 45% in thermal conductivity. Their study reveals that the increase in thermal conductivity improved the heat storage performance of PCM. On the other hand, they monitored the time taken for the temperature to increase from 27 to 31°C. Their results showed that the heat storage and release time decreased compared to the reference sample by about 181 seconds for the heat storage process and 266 seconds for the heat release process. Increasing the thermal conductivity of geopolymer mortars will help the MPCM to charge and discharge its latent heat, thus improving its thermal performance in actual construction.

Figure 15 shows a correlation between the Young's modulus and thermal conductivity of geopolymer mortars at 28 days. A linear correlation expressed by a correlation coefficient R2 = 0.95 is noted. These two properties are dependent on the density of the material, which may explain this linear correlation. A similar correlation between dynamic Young's modulus and thermal conductivity is presented in the study of Barnaure et al. [75] for other material constructions.

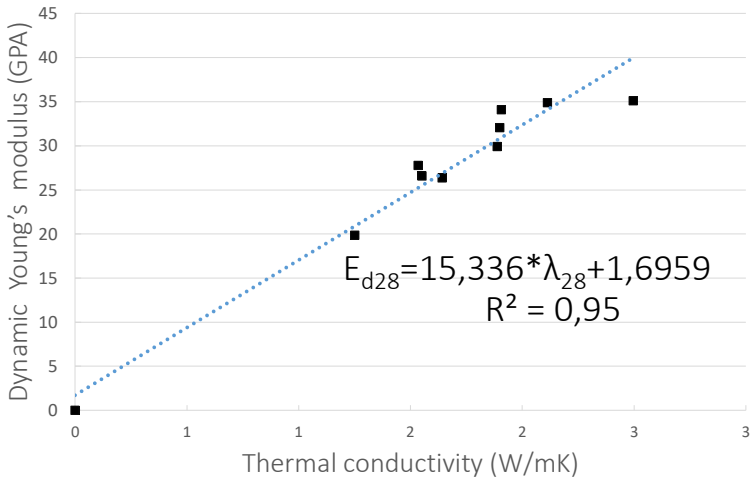

Figure 15. Correlation between dynamic Young's modulus and thermal conductivity at 28 days.

4. Conclusion

The objective of this study was to use the coexistence of two NASH and CASH gels by the inclusion of metakaolin to overcome the negative effects of MPCM incorporation in blast furnace slag-based

665 geopolymer mortars. The conclusions of the different tests after the inclusion of metakaolin are as
666 follows:

667 • The geopolymer-MPCM mortars showed good workability with up to 10% MPCM and 20%
668 MK. The maximum flow time was equal to 4.9 seconds, which is lower than the standard mortar
669 flow time of 7 seconds.
670 • SEM, EDS and XRD analysis confirmed that incorporation of metakaolin into the blast furnace
671 slag matrix produced CASH and NASH gel as stable reaction products.
672 • EDS analysis revealed a higher Si/Al ratio, which means it has the potential to produce a dense
673 and compact bonding geopolymer.
674 • The compressive strength of geopolymer-MPCM mortars is between 49 and 61 MPa and is
675 sufficient for structural applications.

676 • The CASH and NASH gels formed after the addition of MK increased the thermal conductivity,
677 and the latter improved the specific thermal capacity of geopolymer-MPCM mortars. The
678 maximum value obtained is equal to 1280 J/Kg.K This value is higher than the thermal capacity
679 values of Portland cement mortars.

680 Finally, the increase in MPCM rate showed a reduction in mechanical strength and an increase in
681 porosity, which limit the amount of MPCM that can be added to the geopolymer mortar. Future research
682 could focus on developing microcapsules with low agglomeration, excellent compatibility with the
683 concrete matrix and high mechanical strength (robust microcapsule) to overcome these constraints.
684 These could be a viable option to reduce the loss of compressive strength and the increase of porosity.
685 On the other hand, this solution will increase the amount of MPCM in the geopolymer, thus increasing
686 the total thermal energy storage capacity of the geopolymer.

687 **Declaration of Conflict of Interests**

688 The authors declare that they have no known competing financial interests or personal relationships that
689 could have appeared to influence the work reported in this paper.

690 **Credit authorship contribution statement**

Bouha EL MOUSTAPHA: Conceptualization, Methodology, Investigation, Writing - original draft. **Stéphanie BONNET**: Validation, Resources, Visualization, Supervision, review & editing. **Abdelhafid KHELIDJ:** Validation, Resources , Visualization, Supervision, review & editing. **Nordine LEKLOU** : Validation, review & editing. **Daniel FROELICH**: Validation, review & editing , Supervision. **Isselmou AHMEDOU BABAH** : review & editing, Supervision. **Carole CHARBUILLET**: review & editing. **Abderahmane KHALIFA**: Funding acquisition

Acknowledgements

The experimental work was carried out at the Institute of Research in Civil and Mechanical Engineering - CNRS UMR 6183, Saint Nazaire. This experimental work was financed by the Magma laboratory, in this regard we thank the responsible of the Institute of Research in Civil and Mechanical Engineering and the responsible of the Magma laboratory for their support to carry out this study.

Reference

[1] « EFFICIENCY, Energy. Buildings The global exchange for energy efficiency policies, data and analysis: https://www. iea. org/topics/energyefficiency/buildings. 2019. »

[2] S. Drissi, T.-C. Ling, K. H. Mo, et A. Eddhahak, « A review of microencapsulated and composite phase change materials: Alteration of strength and thermal properties of cement-based materials », *Renewable and Sustainable Energy Reviews*, vol. 110, p. 467-484, août 2019, doi: 10.1016/j.rser.2019.04.072.

[3] « SBCI-BCCSummary.pdf ». Accessed: June 10, 2021. [Online]. Available from: http://admin.indiaenvironmentportal.org.in/files/SBCI-BCCSummary.pdf

[4] S. Drissi, T.-C. Ling, et K. H. Mo, « Thermal performance of a solar energy storage concrete panel incorporating phase change material aggregates developed for thermal regulation in buildings », *Renewable Energy*, vol. 160, p. 817-829, nov. 2020, doi: 10.1016/j.renene.2020.06.076.

[5] V. D. Cao *et al.*, « Thermal analysis of geopolymer concrete walls containing microencapsulated phase change materials for building applications », *Solar Energy*, vol. 178, p. 295-307, janv. 2019, doi: 10.1016/j.solener.2018.12.039.

[6] U. Berardi et A. A. Gallardo, « Properties of concretes enhanced with phase change materials for building applications », *Energy and Buildings*, vol. 199, p. 402-414, sept. 2019, doi: 10.1016/j.enbuild.2019.07.014.

[7] V. D. Cao *et al.*, « Microencapsulated phase change materials for enhancing the thermal performance of Portland cement concrete and geopolymer concrete for passive building applications », *Energy Conversion and Management*, vol. 133, p. 56-66, févr. 2017, doi: 10.1016/j.enconman.2016.11.061.

[8] G. Alva, L. Liu, X. Huang, et G. Fang, « Thermal energy storage materials and systems for solar energy applications », *Renewable and Sustainable Energy Reviews*, vol. 68, p. 693-706, févr. 2017, doi: 10.1016/j.rser.2016.10.021.

[9] L. Ventolà, M. Vendrell, et P. Giraldez, « Newly-designed traditional lime mortar with a phase change material as an additive », *Construction and Building Materials*, vol. 47, p. 1210-1216, oct. 2013, doi: 10.1016/j.conbuildmat.2013.05.111.

[10] K.-H. Yang, Y.-B. Jung, M.-S. Cho, et S.-H. Tae, « Effect of supplementary cementitious materials on reduction of CO2 emissions from concrete », *Journal of Cleaner Production*, vol. 103, p. 774-783, sept. 2015, doi: 10.1016/j.jclepro.2014.03.018.

[11] J. Davidovits, « Geopolymer Cement a review 2013 », p. 1-11, janv. 2013.

[12] K. Wang et Iowa State University, Éd., *Proceedings of the International Workshop on Sustainable Development and Concrete Technology, Beijing, China, May 20-21, 2004*. Ames: Center for Transportation Research and Education, Iowa State University, 2004.

[13] C. Carreño-Gallardo *et al.*, « In the CO2 emission remediation by means of alternative geopolymers as substitutes for cements », *Journal of Environmental Chemical Engineering*, vol. 6, n° 4, p. 4878-4884, août 2018, doi: 10.1016/j.jece.2018.07.033.

[14] A. Hasnaoui, E. Ghorbel, et G. Wardeh, « Optimization approach of granulated blast furnace slag and metakaolin based geopolymer mortars », *Construction and Building Materials*, vol. 198, p. 10-26, févr. 2019, doi: 10.1016/j.conbuildmat.2018.11.251.

[15] M. Albitar, M. S. Mohamed Ali, P. Visintin, et M. Drechsler, « Durability evaluation of geopolymer and conventional concretes », *Construction and Building Materials*, vol. 136, p. 374-385, avr. 2017, doi: 10.1016/j.conbuildmat.2017.01.056.

[16] W. G. Valencia Saavedra et R. Mejía de Gutiérrez, « Performance of geopolymer concrete composed of fly ash after exposure to elevated temperatures », *Construction and Building Materials*, vol. 154, p. 229-235, nov. 2017, doi: 10.1016/j.conbuildmat.2017.07.208.

[17] S. A. Bernal et J. L. Provis, « Durability of Alkali-Activated Materials: Progress and Perspectives », *Journal of the American Ceramic Society*, vol. 97, n° 4, p. 997-1008, 2014, doi: 10.1111/jace.12831.

[18] R. Shadnia, L. Zhang, et P. Li, « Experimental study of geopolymer mortar with incorporated PCM », *Construction and Building Materials*, vol. 84, p. 95-102, juin 2015, doi: 10.1016/j.conbuildmat.2015.03.066.

[19] S. Pilehvar *et al.*, « Mechanical properties and microscale changes of geopolymer concrete and Portland cement concrete containing micro-encapsulated phase change materials », *Cement and Concrete Research*, vol. 100, p. 341-349, oct. 2017, doi: 10.1016/j.cemconres.2017.07.012.

[20] S. Pilehvar *et al.*, « Effect of freeze-thaw cycles on the mechanical behavior of geopolymer concrete and Portland cement concrete containing micro-encapsulated phase change materials », *Construction and Building Materials*, vol. 200, p. 94-103, mars 2019, doi: 10.1016/j.conbuildmat.2018.12.057.

[21] V. D. Cao *et al.*, « Influence of microcapsule size and shell polarity on thermal and mechanical properties of thermoregulating geopolymer concrete for passive building applications », *Energy Conversion and Management*, vol. 164, p. 198-209, mai 2018, doi: 10.1016/j.enconman.2018.02.076.

[22] Y. Lin, Y. Jia, G. Alva, et G. Fang, « Review on thermal conductivity enhancement, thermal properties and applications of phase change materials in thermal energy storage », *Renewable and Sustainable Energy Reviews*, vol. 82, p. 2730-2742, févr. 2018, doi: 10.1016/j.rser.2017.10.002.

[23] M. Hunger, A. G. Entrop, I. Mandilaras, H. J. H. Brouwers, et M. Founti, « The behavior of self-compacting concrete containing micro-encapsulated Phase Change Materials », *Cement and Concrete Composites*, vol. 31, n° 10, p. 731-743, nov. 2009, doi: 10.1016/j.cemconcomp.2009.08.002.

[24] A. Jayalath *et al.*, « Properties of cementitious mortar and concrete containing micro-encapsulated phase change materials », *Construction and Building Materials*, vol. 120, p. 408-417, sept. 2016, doi: 10.1016/j.conbuildmat.2016.05.116.

[25] H. Cui, W. Liao, X. Mi, T. Y. Lo, et D. Chen, « Study on functional and mechanical properties of cement mortar with graphite-modified microencapsulated phase-change materials », *Energy and Buildings*, vol. 105, p. 273-284, oct. 2015, doi: 10.1016/j.enbuild.2015.07.043.

[26] Z. Ling, J. Chen, T. Xu, X. Fang, X. Gao, et Z. Zhang, « Thermal conductivity of an organic phase change material/expanded graphite composite across the phase change temperature range and a novel thermal conductivity model », *Energy Conversion and Management*, vol. 102, p. 202-208, sept. 2015, doi: 10.1016/j.enconman.2014.11.040.

[27] T. Xu, Q. Chen, G. Huang, Z. Zhang, X. Gao, et S. Lu, « Preparation and thermal energy storage properties of d-Mannitol/expanded graphite composite phase change material », *Solar Energy Materials and Solar Cells*, vol. 155, p. 141-146, oct. 2016, doi: 10.1016/j.solmat.2016.06.003.

[28] F. Tang, D. Su, Y. Tang, et G. Fang, « Synthesis and thermal properties of fatty acid eutectics and diatomite composites as shape-stabilized phase change materials with enhanced thermal conductivity », *Solar Energy Materials and Solar Cells*, vol. 141, p. 218-224, oct. 2015, doi: 10.1016/j.solmat.2015.05.045.

[29] T. Nomura, K. Tabuchi, C. Zhu, N. Sheng, S. Wang, et T. Akiyama, « High thermal conductivity phase change composite with percolating carbon fiber network », *Applied Energy*, vol. 154, p. 678-685, sept. 2015, doi: 10.1016/j.apenergy.2015.05.042.

[30] M. J. A. Mijarsh, M. A. Megat Johari, et Z. A. Ahmad, « Effect of delay time and Na2SiO3 concentrations on compressive strength development of geopolymer mortar synthesized from TPOFA », *Construction and Building Materials*, vol. 86, p. 64-74, juill. 2015, doi: 10.1016/j.conbuildmat.2015.03.078.

[31] T. Phoo-ngernkham, P. Chindaprasirt, V. Sata, S. Hanjitsuwan, et S. Hatanaka, « The effect of adding nano-SiO2 and nano-Al2O3 on properties of high calcium fly ash geopolymer cured at ambient temperature », *Materials & Design*, vol. 55, p. 58-65, mars 2014, doi: 10.1016/j.matdes.2013.09.049.

[32] C. K. Yip, G. C. Lukey, et J. S. J. van Deventer, « The coexistence of geopolymeric gel and calcium silicate hydrate at the early stage of alkaline activation », *Cement and Concrete Research*, vol. 35, nº 9, p. 1688-1697, sept. 2005, doi: 10.1016/j.cemconres.2004.10.042.

[33] S. A. Bernal, E. D. Rodríguez, R. Mejía de Gutiérrez, M. Gordillo, et J. L. Provis, « Mechanical and thermal characterisation of geopolymers based on silicate-activated metakaolin/slag blends », *J Mater Sci*, vol. 46, nº 16, p. 5477-5486, août 2011, doi: 10.1007/s10853-011-5490-z.

[34] S. A. Bernal, R. Mejía de Gutiérrez, et J. L. Provis, « Engineering and durability properties of concretes based on alkali-activated granulated blast furnace slag/metakaolin blends », *Construction and Building Materials*, vol. 33, p. 99-108, août 2012, doi: 10.1016/j.conbuildmat.2012.01.017.

[35] M. Kamath, S. Prashant, et M. Kumar, « Micro-characterisation of alkali activated paste with fly ash-GGBS-metakaolin binder system with ambient setting characteristics », *Construction and Building Materials*, vol. 277, p. 122323, mars 2021, doi: 10.1016/j.conbuildmat.2021.122323.

[36] T. Phoo-ngernkham, V. Sata, S. Hanjitsuwan, C. Ridtirud, S. Hatanaka, et P. Chindaprasirt, « High calcium fly ash geopolymer mortar containing Portland cement for use as repair material », *Construction and Building Materials*, vol. 98, p. 482-488, nov. 2015, doi: 10.1016/j.conbuildmat.2015.08.139.

[37] G. F. Huseien, J. Mirza, M. Ismail, M. W. Hussin, M. A. M. Arrifin, et A. A. Hussein, « The Effect of Sodium Hydroxide Molarity and Other Parameters on Water Absorption of Geopolymer Mortars », *Indian Journal of Science and Technology*, vol. 9, nº 48, déc. 2016, doi: 10.17485/ijst/2016/v9i48/109629.

[38] S. Pilehvar *et al.*, « Physical and mechanical properties of fly ash and slag geopolymer concrete containing different types of micro-encapsulated phase change materials », *Construction and Building Materials*, vol. 173, p. 28-39, juin 2018, doi: 10.1016/j.conbuildmat.2018.04.016.

825 [39] « EN 196-1. Methods of testing cement- Part 1: Determination of strength. European committee for
826 standardization, 2016. »
827 [40] S. Ahmari, X. Ren, V. Toufigh, et L. Zhang, « Production of geopolymeric binder from blended
828 waste concrete powder and fly ash », *Construction and Building Materials*, vol. 35, p. 718-729, oct.
829 2012, doi: 10.1016/j.conbuildmat.2012.04.044.
830 [41] « AFNOR NF P18-452, Bétons – Measurement of the flow time of concrete and mortar with the
831 maniabilimeter, AFNOR Editions, 2017. »
832 [42] « NF P 18-459. Concrete – Testing Hardened Concrete-Testing Porosity and Density. French
833 Association for Standardization AFNOR 2010. »
834 [43] « ASTM E1876 – 15, Standard Test Method for Dynamic Young's Modulus, Shear Modulus and
835 Poisson's Ratio by Impulse Excitation of Vibration, n.d. »
836 [44] Y. He, « Rapid thermal conductivity measurement with a hot disk sensor: Part 1. Theoretical
837 considerations », *Thermochimica Acta*, vol. 436, n° 1, p. 122-129, oct. 2005, doi:
838 10.1016/j.tca.2005.06.026.
839 [45] C. Fabiani et A. L. Pisello, « Coupling controlled environmental forcing and transient plane source
840 method: An innovative thermal characterization procedure for building insulation materials »,
841 *Applied Thermal Engineering*, vol. 130, p. 254-263, févr. 2018, doi:
842 10.1016/j.applthermaleng.2017.10.155.
843 [46] J. Zhang, C. Shi, Z. Zhang, et Z. Ou, « Durability of alkali-activated materials in aggressive
844 environments: A review on recent studies », *Construction and Building Materials*, vol. 152, p.
845 598-613, oct. 2017, doi: 10.1016/j.conbuildmat.2017.07.027.
846 [47] P. Chindaprasirt, T. Chareerat, et V. Sirivivatnanon, « Workability and strength of coarse high
847 calcium fly ash geopolymer », *Cement and Concrete Composites*, vol. 29, n° 3, p. 224-229, mars
848 2007, doi: 10.1016/j.cemconcomp.2006.11.002.
849 [48] M. N. S. Hadi, H. Zhang, et S. Parkinson, « Optimum mix design of geopolymer pastes and
850 concretes cured in ambient condition based on compressive strength, setting time and workability »,
851 *Journal of Building Engineering*, vol. 23, p. 301-313, mai 2019, doi: 10.1016/j.jobe.2019.02.006.

[49] P. S. Deb, P. Nath, et P. K. Sarker, « The effects of ground granulated blast-furnace slag blending with fly ash and activator content on the workability and strength properties of geopolymer concrete cured at ambient temperature », *Materials & Design (1980-2015)*, vol. 62, p. 32-39, oct. 2014, doi: 10.1016/j.matdes.2014.05.001.

[50] P. N. Lemougna *et al.*, « Effect of slag on the improvement of setting time and compressive strength of low reactive volcanic ash geopolymers synthetized at room temperature », *Materials Chemistry and Physics*, vol. 239, p. 122077, janv. 2020, doi: 10.1016/j.matchemphys.2019.122077.

[51] M. Ibrahim, M. A. M. Johari, M. Maslehuddin, et M. K. Rahman, « Influence of nano-SiO2 on the strength and microstructure of natural pozzolan based alkali activated concrete », *Construction and Building Materials*, vol. 173, p. 573-585, juin 2018, doi: 10.1016/j.conbuildmat.2018.04.051.

[52] P. S. Deb, P. K. Sarker, et S. Barbhuiya, « Effects of nano-silica on the strength development of geopolymer cured at room temperature », *Construction and Building Materials*, vol. 101, p. 675-683, déc. 2015, doi: 10.1016/j.conbuildmat.2015.10.044.

[53] G. F. Huseien, J. Mirza, M. Ismail, S. K. Ghoshal, et M. A. M. Ariffin, « Effect of metakaolin replaced granulated blast furnace slag on fresh and early strength properties of geopolymer mortar », *Ain Shams Engineering Journal*, vol. 9, nº 4, p. 1557-1566, déc. 2018, doi: 10.1016/j.asej.2016.11.011.

[54] J. L. Provis et S. A. Bernal, « Geopolymers and Related Alkali-Activated Materials », *Annual Review of Materials Research*, vol. 44, nº 1, p. 299-327, 2014, doi: 10.1146/annurev-matsci-070813-113515.

[55] M. J. A. Mijarsh, M. A. Megat Johari, et Z. A. Ahmad, « Synthesis of geopolymer from large amounts of treated palm oil fuel ash: Application of the Taguchi method in investigating the main parameters affecting compressive strength », *Construction and Building Materials*, vol. 52, p. 473-481, févr. 2014, doi: 10.1016/j.conbuildmat.2013.11.039.

[56] Y. J. Zhang, Y. C. Wang, D. L. Xu, et S. Li, « Mechanical performance and hydration mechanism of geopolymer composite reinforced by resin », *Materials Science and Engineering: A*, vol. 527, nº 24, p. 6574-6580, sept. 2010, doi: 10.1016/j.msea.2010.06.069.

[57] K. Kupwade-Patil et E. Allouche, « Effect of Alkali Silica Reaction (ASR) in Geopolymer Concrete », p. 12.

[58] A. Mobili, A. Belli, C. Giosuè, A. Telesca, M. Marroccoli, et F. Tittarelli, « Calcium Sulfoaluminate, Geopolymeric, and Cementitious Mortars for Structural Applications », *Environments*, vol. 4, nº 3, Art. nº 3, sept. 2017, doi: 10.3390/environments4030064.

[59] M. Yang, S. R. Paudel, et E. Asa, « Comparison of pore structure in alkali activated fly ash geopolymer and ordinary concrete due to alkali-silica reaction using micro-computed tomography », *Construction and Building Materials*, vol. 236, p. 117524, mars 2020, doi: 10.1016/j.conbuildmat.2019.117524.

[60] T. Bai, Z.-G. Song, Y.-G. Wu, X.-D. Hu, et H. Bai, « Influence of steel slag on the mechanical properties and curing time of metakaolin geopolymer », *Ceramics International*, vol. 44, nº 13, p. 15706-15713, sept. 2018, doi: 10.1016/j.ceramint.2018.05.243.

[61] A. Nazari et J. G. Sanjayan, « Synthesis of geopolymer from industrial wastes », *Journal of Cleaner Production*, vol. 99, p. 297-304, juill. 2015, doi: 10.1016/j.jclepro.2015.03.003.

[62] B. B. Sabir, S. Wild, et J. Bai, « Metakaolin and calcined clays as pozzolans for concrete: a review », *Cement and Concrete Composites*, vol. 23, nº 6, p. 441-454, déc. 2001, doi: 10.1016/S0958-9465(00)00092-5.

[63] P. D. Silva, K. Sagoe-Crenstil, et V. Sirivivatnanon, « Kinetics of geopolymerization: Role of Al2O3 and SiO2 », *Cement and Concrete Research*, vol. 37, nº 4, p. 512-518, avr. 2007, doi: 10.1016/j.cemconres.2007.01.003.

[64] I. Lecomte, C. Henrist, M. Liégeois, F. Maseri, A. Rulmont, et R. Cloots, « (Micro)-structural comparison between geopolymers, alkali-activated slag cement and Portland cement », *Journal of the European Ceramic Society*, vol. 26, nº 16, p. 3789-3797, janv. 2006, doi: 10.1016/j.jeurceramsoc.2005.12.021.

[65] P. Duxson, J. L. Provis, G. C. Lukey, S. W. Mallicoat, W. M. Kriven, et J. S. J. van Deventer, « Understanding the relationship between geopolymer composition, microstructure and mechanical properties », *Colloids and Surfaces A: Physicochemical and Engineering Aspects*, vol. 269, nº 1, p. 47-58, nov. 2005, doi: 10.1016/j.colsurfa.2005.06.060.

907 [66] A. Mobili, A. Belli, C. Giosuè, T. Bellezze, et F. Tittarelli, « Metakaolin and fly ash alkali-activated
908 mortars compared with cementitious mortars at the same strength class », *Cement and Concrete*
909 *Research*, vol. 88, p. 198-210, oct. 2016, doi: 10.1016/j.cemconres.2016.07.004.
910 [67] B. Šavija, H. Zhang, et E. Schlangen, « Influence of Microencapsulated Phase Change Material
911 (PCM) Addition on (Micro) Mechanical Properties of Cement Paste », *Materials*, vol. 10, nº 8, Art.
912 nº 8, août 2017, doi: 10.3390/ma10080863.
913 [68] G. Samson, M. Cyr, et X. X. Gao, « Formulation and characterization of blended alkali-activated
914 materials based on flash-calcined metakaolin, fly ash and GGBS », *Construction and Building*
915 *Materials*, vol. 144, p. 50-64, juill. 2017, doi: 10.1016/j.conbuildmat.2017.03.160.
916 [69] A. Mobili, C. Giosuè, M. Bitetti, et F. Tittarelli, « Cement mortars and geopolymers with the same
917 strength class », *Proceedings of the Institution of Civil Engineers - Construction Materials*, vol.
918 169, nº 1, p. 3-12, févr. 2016, doi: 10.1680/coma.14.00063.
919 [70] J. L. Provis, R. J. Myers, C. E. White, V. Rose, et J. S. J. van Deventer, « X-ray microtomography
920 shows pore structure and tortuosity in alkali-activated binders », *Cement and Concrete Research*,
921 vol. 42, nº 6, p. 855-864, juin 2012, doi: 10.1016/j.cemconres.2012.03.004.
922 [71] P. H. R. Borges, N. Banthia, H. A. Alcamand, W. L. Vasconcelos, et E. H. M. Nunes, « Performance
923 of blended metakaolin/blastfurnace slag alkali-activated mortars », *Cement and Concrete*
924 *Composites*, vol. 71, p. 42-52, août 2016, doi: 10.1016/j.cemconcomp.2016.04.008.
925 [72] K. Sasaguchi et R. Viskanta, « Phase Change Heat Transfer During Melting and Resolidification of
926 Melt Around Cylindrical Heat Source(s)/Sink(s) », *Journal of Energy Resources Technology*, vol.
927 111, nº 1, p. 43-49, mars 1989, doi: 10.1115/1.3231400.
928 [73] K. Cellat *et al.*, « 2 years of monitoring results from passive solar energy storage in test cabins with
929 phase change materials », *Solar Energy*, vol. 200, p. 29-36, avr. 2020, doi:
930 10.1016/j.solener.2019.01.045.
931 [74] B. Xu et Z. Li, « Paraffin/diatomite/multi-wall carbon nanotubes composite phase change material
932 tailor-made for thermal energy storage cement-based composites », *Energy*, vol. 72, p. 371-380,
933 août 2014, doi: 10.1016/j.energy.2014.05.049.

[75] M. Barnaure, S. Bonnet, et P. Poullain, « Earth buildings with local materials: Assessing the variability of properties measured using non-destructive methods », *Construction and Building Materials*, vol. 281, p. 122613, avr. 2021, doi: 10.1016/j.conbuildmat.2021.122613.